# Dalton Transactions

Accepted Manuscript






ROYAL SOCIETY OF CHEMISTRY

www.rsc.org/dalton

Journal Name

ARTICLE

# Reactions of alkynes with *cis*-$RuCl_2(dppm)_2$: exploring the interplay of vinylidene, alkynyl and $\eta^3$-butenynyl complexes

Received 00th January 20xx,
Accepted 00th January 20xx

DOI: 10.1039/x0xx00000x

www.rsc.org/

Samantha G. Eaves,[a,b] Dmitry S. Yufit,[a] Brian W. Skelton,[c] Jason M. Lynam[d] and Paul J. Low[b]

Reactions of *cis*-$RuCl_2(dppm)_2$ with various terminal alkynes, of the type $HC{\equiv}CC_6H_4$-4-R (1 equiv.), in the presence of $TlBF_4$ have resulted in the formation of cationic vinylidene complexes *trans*-[RuCl(=C=$CHC_6H_4$-4-R)$(dppm)_2$]$BF_4$ ([**1**]$BF_4$). These complexes can be isolated, or treated *in situ* with a suitable base (Proton Sponge, 1,8-*bis*-dimethylaminonapthalene) to yield the *mono*-alkynyl complexes *trans*-RuCl(C≡$CC_6H_4$-4-R)$(dppm)_2$ (**2**). Through similar reactions between *cis*-$RuCl_2(dppm)_2$ with 2 equiv. of alkyne, $TlBF_4$ and base, *trans*-bis(alkynyl) complexes, *trans*-Ru(C≡$CC_6H_4$-4-R)$_2(dppm)_2$ (**3**), can be isolated when R is an electron withdrawing substituent (R = $NO_2$, COOMe, C≡$CSiMe_3$), whereas reactions with alkynes bearing electron donating substituents (R = OMe and Me) form cationic $\eta^3$-butenynyl complexes [Ru($\eta^3$-{HC($C_6H_4$-4-R)=CC≡$CC_6H_4$-4-R})$(dppm)_2]^+$ ([**4**]$^+$). This work highlights the importance of the electronic character of the alkyne in governing product outcome.

## Introduction

Ruthenium alkynyl complexes of the type *trans*-Ru(C≡CR´)$_2(dppe)_2$ have begun to attract considerable interest as potential components in the area of molecular electronics,[1-6] due to the extensive Ru(d)-C≡C(π) frontier orbital mixing,[7] wire-like behaviour,[1, 5, 8-10] and facile synthesis from *cis*-$RuCl_2(dppe)_2$[11, 12] or five-coordinate [RuCl$(dppe)_2$]X (X = $PF_6$, OTf).[13-15] The incorporation of a metal fragment within the conjugated π-system also allows tuning of the orbital energies to better match the electrode Fermi levels, leading to higher conduction values across a junction.[7, 16-21] Several studies have explored the influence of the nature and length of the alkynyl fragments and surface binding groups.[1, 5, 9, 18, 22-25] However, given the importance the ancillary equatorial ligands might play in tuning solubility, redox potentials and chemical stability, optimisation of these supporting ligands should also be an important consideration within the molecular design.

In seeking to explore the influence of supporting ligands on the molecular electronic properties of *trans*-*bis*(alkynyl) complexes of ruthenium, we have focussed attention on complexes *trans*-Ru(C≡CR´)$_2(dppm)_2$, complementing studies on related complexes based on *trans*-Ru(C≡CR´)$_2(dppe)_2$[3, 26] and *trans*-Fe(C≡CR´)$_2(depe)_2$.[18, 22, 27] Earlier reports have described the preparation of such complexes from *cis*-$RuCl_2(dppm)_2$, or the intermediate *mono*-alkynyl complexes *trans*-RuCl(C≡CR´)$(dppm)_2$, and terminal alkynes in the presence of $NaPF_6$ and various bases in reactions that take place over 12 – 24 hours, although yields are often low (< 30%), especially in the case of alkynes bearing electron-donating substituents.[28-30] Trimethylstannylalkynes have also been used in related transformations employing a CuI catalyst.[31-33] However the difficulty in the activation of the second chloride from *trans*-RuCl(C≡CR´)$(dppm)_2$ has been noted.[34] Furthermore, reactions of *cis*-$RuCl_2(dppm)_2$ with more than one equivalent of alkyl or phenyl acetylenes and $NaPF_6$ in methanol result in the formation of $\eta^3$-butenynyl products.[35]

We report here a rapid synthetic protocol for the preparation of *trans*-Ru(C≡$CC_6H_4$-4-R)$_2(dppm)_2$ complexes from *cis*-$RuCl_2(dppm)_2$ and HC≡$CC_6H_4$-4-R in the presence of $TlBF_4$ and a suitable base (1,8-*bis*-dimethylaminonaphthalene, Proton Sponge) in $CH_2Cl_2$ solutions, and describe the influence of the alkynyl substituents in directing the product distribution between *trans*-bis(alkynyl) and $\eta^3$-butenynyl complexes.

## Results

### Syntheses

Reactions of $CH_2Cl_2$ solutions of *cis*-$RuCl_2(dppm)_2$ with various terminal alkynes of the type $HC{\equiv}CC_6H_4$-4-R (1 equiv.) and $TlBF_4$ (1 equiv.) result in the formation of vinylidene complexes *trans*-[RuCl(=C=$CHC_6H_4$-4-R)$(dppm)_2$]$BF_4$ [R = $NO_2$ ([**1a**]$BF_4$), COOMe ([**1b**]$BF_4$), C≡$CSiMe_3$ ([**1c**]$BF_4$), H ([**1d**]$BF_4$), Me ([**1e**]$BF_4$) and OMe ([**1f**]$BF_4$) over 1 – 2 hours (Scheme 1). The complexes can be isolated in high yields (66 – 83 %) by simple

[a] Department of Chemistry, Durham University, South Road, Durham DH1 3LE, UK.
[b] School of Chemistry and Biochemistry, The University of Western Australia, 35 Stirling Highway, Perth, Western Australia 6009, e-mail paul.low@uwa.edu.au tel (+61 8) 6488 3045.
[c] Centre for Microscopy, Characterisation and Analysis, University of Western Australia, 35 Stirling Highway, Perth, Western Australia 6009, Australia.
[d] Department of Chemistry, University of York, Heslington, York, YO10 5DD, e-mail jason.lynam@york.ac.uk tel +44(0)1904322534

Electronic Supplementary Information (ESI) available: Detailed experimental procedures and characterisation. Summary of molecular structures. Crystallographic data in CIF format are available from the CCDC 1426045-1426051. Computational details, energies, atom coordinates and frequencies. See DOI: 10.1039/x0xx00000x

filtration (to remove TlCl) and precipitation (see Supporting Information). Evidence for the formation of [**1**]$^+$ include quintet (or multiplet) resonances for the vinylidene protons between δ 2.94 – 3.36 ppm, with a $^4J_{PH}$ coupling of 3 Hz in the $^1$H NMR spectra. In the $^{13}C\{^1H\}$ NMR spectra, low field resonances for the Ru=*C* carbon nuclei (δ 352.5 – 362.6 ppm) (Table 1), displaying coupling to the four *cis*-phosphines, and singlet resonances for the Ru=C=*C* carbon nuclei (δ 109.4 – 111.1 ppm) confirm the presence of the vinylidene ligand. In the IR spectra, the observation of ν(Ru=C=C) bands (1605 – 1653 cm$^{-1}$) further support the presence of a vinylidene ligand.

**Table 1:** Selected $^{13}C\{^1H\}$ NMR spectroscopy data (ppm) for vinylidene ([**1**]$^+$) ($CD_2Cl_2$) and *mono*-alkynyl (**2**) complexes ($CDCl_3$).

| Complex | | [1]$^+$ | | 2 | |
|---|---|---|---|---|---|
| | R | $C_\alpha$ / ppm | $^2J_{CP}$ / Hz | $C_\alpha$ / ppm | $^2J_{CP}$ / Hz |
| **a** | $NO_2$ | 352.5 | 14 | 147.6 | 16 |
| **b** | COOMe | 355.4 | 14 | 144.8 | *a* |
| **c** | C≡CSiMe$_3$ | 356.0 | *a* | 130.8 | 15 |
| **d** | H | 358.2 | 13 | 123.0 | 15 |
| **e** | Me | 359.5 | 15 | 120.4 | 15 |
| **f** | OMe | 362.5 | *a* | 118.2 | 15 |

*a* multiplet, coupling unresolved.

These vinylidene complexes serve as convenient intermediates in the preparation of the analogous acetylide complexes in the usual fashion. Following formation of [**1**]$BF_4$ *in situ* and filtration to remove the precipitated Tl(I) salts, addition of 1,8-*bis*-dimethylaminonapthalene immediately yields the *mono*-alkynyl complexes *trans*-RuCl(C≡C$C_6H_4$-4-R)(dppm)$_2$ (**2**) in high yields (74 – 92 %; R = $NO_2$ (**2a**), COOMe (**2b**), C≡CSiMe$_3$ (**2c**), H (**2d**), Me (**2e**) and OMe (**2f**)) (Scheme 1). Due to the strongly π-accepting nature of the vinylidene ligand, abstraction of the *trans*-chloride from [**1**]$^+$ (the preliminary step in forming *bis*-alkynyl complexes, vide infra) is slow, allowing selective formation of the *mono*-vinylidene and subsequent *mono*-acetylide products. However, failure to control the 1:1:1 *cis*-$RuCl_2$(dppm)$_2$ : $TlBF_4$ : alkyne stoichiometry, or failure to allow complete formation of the *mono*-vinylidene before addition of the base, results in contamination of the product by the *trans*-bis(alkynyl) complex *trans*-Ru(C≡C$C_6H_4$-4-R)$_2$(dppm)$_2$, which is difficult to separate.

In the $^{13}C\{^1H\}$ NMR spectra of **2**, quintet (or multiplet resonances) for the Ru-*C* carbon nuclei (δ 118.2 – 147.6 ppm) (Table 1) and singlet resonances for the Ru-C≡*C* carbon nuclei (δ 111.9 – 117.0 ppm) confirm the presence of the alkynyl ligand. In the IR spectra, ν(RuC≡C) bands were observed between 2058 – 2083 cm$^{-1}$. Finally, the structures of **2b – f** have been determined by single crystal X-ray diffraction studies, the structure of **2a** having been previously reported,[36] which confirm the structural assignments.

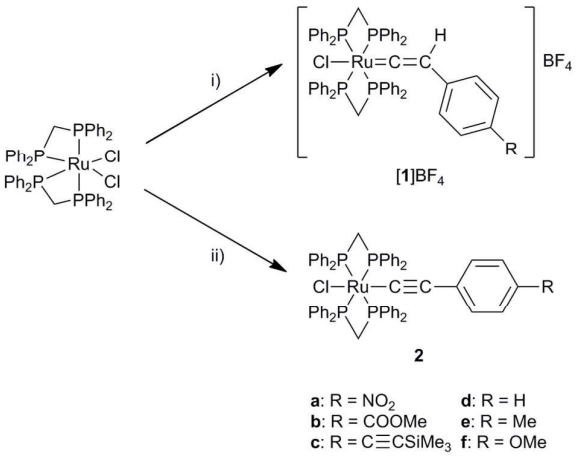


**Scheme 1:** Formation of vinylidene ([**1**]$BF_4$) and *mono*-alkynyl (**2**) Ru(dppm)$_2$ complexes, where i) $TlBF_4$ (1 equiv.), HC≡C$C_6H_4$-4-R (1 equiv.); ii) $TlBF_4$ (1 equiv.), HC≡C$C_6H_4$-4-R (1 equiv.), 1,8-*bis*-dimethylaminonapthalene (excess), in $CH_2Cl_2$ solutions.

One-pot reactions of *cis*-$RuCl_2$(dppm)$_2$ with $TlBF_4$ (2 equiv.), HC≡C$C_6H_4$-4-R (2.2 equiv.; R = $NO_2$ (**3a**), COOMe (**3b**) and C≡CSiMe$_3$ (**3c**)) and 1,8-*bis*-dimethylaminonapthalene (excess) in $CH_2Cl_2$ solutions allowed the isolation of *trans*-bis(alkynyl) complexes *trans*-Ru(C≡C$C_6H_4$-4-R)$_2$(dppm)$_2$ (**3**) in moderate to good yields (48 – 80 %) and after prolonged reaction times (16 hours – 3.5 days) (Scheme 2). For complexes **3a – c**, in the $^{13}C\{^1H\}$ NMR spectra multiplet resonances for the Ru-*C* carbon nuclei (δ 136.7 – 150.1 ppm) and singlet resonances for the Ru-C≡*C* carbon nuclei (δ 116.2 – 119.0 ppm) together with ν(RuC≡C) bands between 2053 – 2062 cm$^{-1}$ in the IR spectra confirm the presence of the alkynyl ligands. The structure of **3b** has been determined by single crystal X-ray diffraction, the structure of **3a** having been previously reported.[37]

However, in contrast to the reactions yielding **3a – c**, analogous one-pot reactions of *cis*-$RuCl_2$(dppm)$_2$ with more electron-rich alkynes HC≡C$C_6H_4$-4-R (2.2 equiv.) gave cationic η$^3$-butenynyl complexes [Ru(η$^3$-{HC($C_6H_4$-4-R)=CC≡C$C_6H_4$-4-R})(dppm)$_2$]$BF_4$ ([**4**]$BF_4$) (R = Me [**4e**]$^+$, OMe [**4f**]$^+$) (Scheme 2).[35]

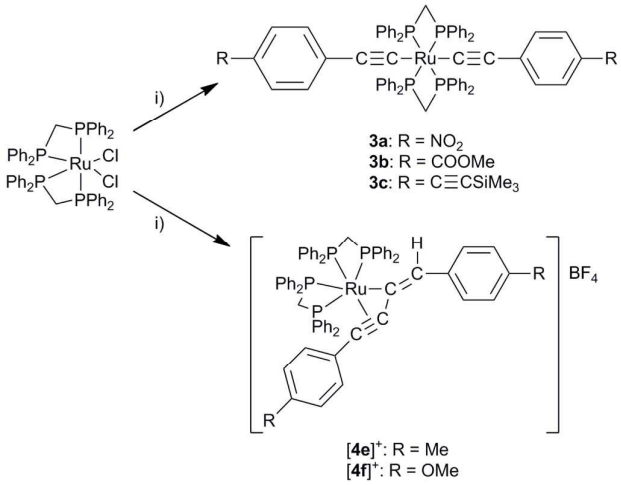


**Scheme 2:** Formation of *trans*-bis(alkynyl), **3**, and $\eta^3$-butenynyl [**4**]$^+$ Ru(dppm)$_2$ complexes, where i) $TlBF_4$ (2 equiv.), $HC{\equiv}CC_6H_4$-4-R (2.2 equiv.) and 1,8-*bis*-dimethylaminonapthalene (excess) in $CH_2Cl_2$ solution.

Evidence for the formation of [**4**]$^+$ includes the observation of four ddd resonances in the $^{31}P\{^1H\}$ NMR spectra, showing a large $^2J_{PP}$ coupling constant (318 Hz, [**4e**]$^+$; 322 Hz, [**4f**]$^+$) from the four inequivalent phosphorus atoms, two of which are in a mutually *trans* disposition. In the $^1H$ NMR spectra singlet resonances for the methyl protons were observed at δ 2.34, [**4e**]$^+$ and δ 3.81 ppm [**4f**]$^+$ and doublet resonances for the vinyl protons were observed at δ 5.55, [**4e**]$^+$ and δ 5.53 ppm, [**4f**]$^+$, with a $^4J_{PH}$ coupling of 5 Hz. The coordination of the alkyne group to the metal centre was confirmed by doublet resonances at δ 108.7, [**4e**]$^+$ and δ 108.5 ppm, [**4f**]$^+$, in the $^{13}C\{^1H\}$ NMR spectra for $C^1$ (for atom labelling see Figure 3) with $^2J_{CP}$ coupling of 22 Hz. Furthermore, the structure of [**4e**]$^+$ (Figure 3) has been determined by a single crystal X-ray diffraction study.

### X-ray Crystallography

Single crystal structure determinations have been made for **2b – f**, **3b** and [**4e**]$^+$, with important bond lengths and angles summarised in Tables 2 and 3, together with those of **2a**[36] and **3a**[37] for comparison and completeness. Crystal data and plots of each of these molecules are given in the Supporting Information, and the atom labelling scheme is summarised in Figure 1.

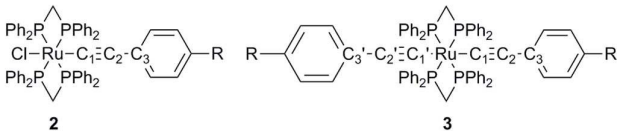


**Figure 1**. The atom labelling scheme used in Table 1 and Table 2.

**Table 2:** Selected bond distances (Å) and torsion angles (θ / °) for: *trans*-RuCl(C≡CC$_6$H$_4$-4-COOMe)(dppm)$_2$ (**2b**); *trans*-RuCl(C≡CC$_6$H$_4$-4-C≡CSiMe$_3$)(dppm)$_2$ (**2c**); *trans*-RuCl(C≡CC$_6$H$_5$)(dppm)$_2$ (**2d**); *trans*-RuCl(C≡CC$_6$H$_4$-4-Me)(dppm)$_2$ (**2e**); *trans*-RuCl(C≡CC$_6$H$_4$-4-OMe)(dppm)$_2$ (**2f**) and *trans*-Ru(C≡CC$_6$H$_4$-4-COOMe)$_2$(dppm)$_2$ (**3b**) (this work) with *trans*-RuCl(C≡CC$_6$H$_4$-4-NO$_2$)(dppm)$_2$ (**2a**)[36] and *trans*-Ru(C≡CC$_6$H$_4$-4-NO$_2$)$_2$(dppm)$_2$ (**3a**)[37] for reference.

| | Ru-C$^1$ | C$^1$≡C$^2$ | C$^2$-C$^3$ | Ru-Cl | Ru-P$^{1-4}$ | θ |
|---|---|---|---|---|---|---|
| **2a**[36] | 1.998(7) | 1.190(8) | 1.428(8) | 2.483(2) | 2.332(2), 2.379(2), 2.332(2), 2.358(2) | 84.1 |
| **2b** | 2.019(3) | 1.181(4) | 1.464(4) | 2.4862(7) | 2.3427(7), 2.3692(7), 2.3247(7), 2.3678(6) | 92.5 |
| **2c** | 2.010(3) | 1.187(4) | 1.432(4) | 2.4629(8) | 2.3404(7), 2.3138(8), 2.3302(7), 2.3593(8) | 9.1 |
| **2d** | 2.004(1) | 1.201(3) | 1.436(3) | 2.4511(4) | 2.3445(5), 2.3454(5), 2. 32055), 2.3557(5) | 25.3 |
| **2e** | 1.999(4) | 1.221(5) | 1.427(5) | 2.4938(9) | 2.3487(8), 2.3358(8), 2.3312(8), 2.3744(8) | 82.3 |
| **2f** | 2.014(9) | 1.15(1) | 1.45(1) | 2.558(2) | 2.338(2), 2.315(2), 2.348(2), 2.347(2) | 2.7 |
| **3a**[37] | 2.051(3) | 1.207(4) | 1.427(5) | - | 2.344(1), 2.344(1), 2.3341(9), 2.3341(9) | 13.8 |
| **3b** | 2.085(6) | 1.150(7) | 1.457(8) | - | 2.331(2), 2.360(1), 2.331(1), 2.360(1) | 80.3 |

**Table 3**: Selected bond angles (°) for: *trans*-RuCl(C≡CC$_6$H$_4$-4-COOMe)(dppm)$_2$ (**2b**); *trans*-RuCl(C≡CC$_6$H$_4$-4-C≡CSiMe$_3$)(dppm)$_2$ (**2c**); *trans*-RuCl(C≡CC$_6$H$_5$)(dppm)$_2$ (**2d**); *trans*-RuCl(C≡CC$_6$H$_4$-4-Me)(dppm)$_2$ (**2e**); *trans*-RuCl(C≡CC$_6$H$_4$-4-OMe)(dppm)$_2$ (**2f**) and *trans*-Ru(C≡CC$_6$H$_4$-4-COOMe)$_2$(dppm)$_2$ (**3b**) (this work) with *trans*-RuCl(C≡CC$_6$H$_4$-4-NO$_2$)(dppm)$_2$ (**2a**)[36] and *trans*-Ru(C≡CC$_6$H$_4$-4-NO$_2$)$_2$(dppm)$_2$ (**3a**)[37] for reference.

| | Cl-Ru-C$^1$ | Ru-C$^1$-C$^2$ | C$^1$-C$^2$-C$^3$ | P$^1$-Ru-P$^4$ | P$^2$-Ru-P$^3$ |
|---|---|---|---|---|---|
| **2a**[36] | 177.7(2) | 176.8(5) | 168.4(7) | 177.90(6) | 177.15(6) |
| **2b** | 175.30(7) | 175.5(2) | 172.9(3) | 178.03(2) | 177.72(2) |
| **2c** | 173.83(9) | 173.9(3) | 177.7(4) | 177.09(3) | 176.31(3) |
| **2d** | 177.91(5) | 177.41(17) | 175.2(2) | 174.35(2) | 178.89(2) |
| **2e** | 173.9(1) | 175.5(3) | 172.5(4) | 177.02(3) | 177.31(3) |
| **2f** | 174.7(2) | 177.8(8) | 169.1(1) | 179.05(9) | 179.88(1) |
| **3a**[37] | 180[a] | 178.3(3) | 173.9(4) | 180 | 180 |
| **3b** | 180[a] | 177.7(5) | 172.0(6) | 180 | 180 |

[a] for Cl read C(X)

The P-Ru-P bond angles between *cis*-phosphines (*ca.* 70 °) and those between *trans*-phosphines (*ca.* 178 °) and Cl/C-Ru-C≡ angles (173.83 – 180 °), indicate the octahedral geometry about the ruthenium centre, which is in agreement with similar structures (**2a** and **3a**) reported earlier.[36, 37] The bond angles along the 5-atom Cl-Ru-C$^1$≡C$^2$-C$^3$- and –C$^1$'-Ru-C$^1$≡C$^2$-C$^3$- chains are close to 180 ° with slight deviations that can be attributed to molecular packing and steric effects.

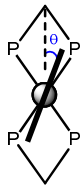


**Figure 2:** Representation of angle θ in *trans*-RuCl(C≡CC$_6$H$_4$-4-R)(dppm)$_2$ (**2**) and *trans*-Ru(C≡CC$_6$H$_4$-4-R)$_2$(dppm)$_2$ (**3**) complexes

The alkynyl ligand is a notoriously insensitive structural probe of electronic character, with only a small contribution from π-backbonding to the bonding in these ligands.[38] Furthermore, even this small contribution is sensitive to the orientation adopted by the phenylene ring system relative to the metal fragment which determines the effectiveness of ligand (π / π*) / metal (d) orbital overlaps.[1] The angle θ (Figure 2) provides a convenient proxy measure for the alignment of the aryl π-system with the metal d-orbitals on geometric grounds. Angles close to 0° or 90° giving rise to the most effective overlaps and hence greatest correlation of structural and electronic properties.[1] The Ru-Cl distance also provides an alternative geometric measure for the electronic properties of the ligands in these systems (Table 2). In complexes **2a** and **2b** bearing electron-withdrawing R groups, the Ru-Cl distances cluster at the shorter end of the range, whilst those from **2e** and **2f** bearing the more electron-rich tolyl and anisole rings are significantly longer. These complexes adopt conformations in the solid state with θ angles close to the idealised values. However, less clear trends in Ru-Cl bond lengths with nature of the aryl substituent are observed for **2c** (θ = 10°) and **2d** (θ = 25°). Similarly, **2e** and **2f** have, on average, shorter Ru-P bond lengths than **2a** and **2b** (by *ca.* 0.01 Å) consistent with increased Ru-P back-bonding arising from increased σ-donation to the metal from the alkynyl fragments.

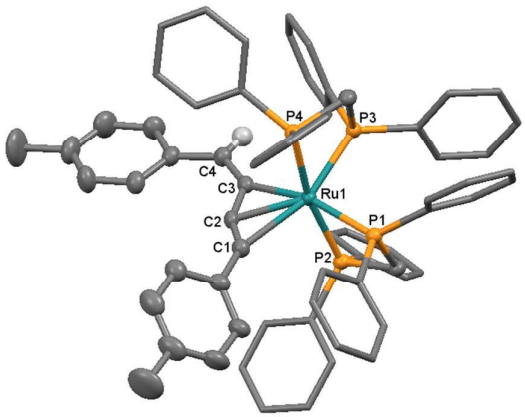


**Figure 3:** A plot of the cation [**4e**]$^+$ with solvent of crystallisation (0.5 × C$_3$H$_6$O), counter ion ([BF$_4$]$^-$) and selected hydrogen atoms removed for clarity. Selected bond lengths / Å: C(1)-C(2) 1.259(5) Å; C(2)-C(3) 1.367(5) Å; C(3)-C(4) 1.343(5) Å; P(1)-Ru(1) 2.3723(10) Å; P(2)-Ru(1) 2.3497(9) Å; P(3)-Ru(1) 2.3128(8) Å; P(4)-Ru(1) 2.3685(9) Å; Ru(1)-C(1) 2.387(3) Å; Ru(1)-C(2) 2.208(3) Å; Ru(1)-C(3) 2.136(4) Å and selected bond angles / °: C(1)-C(2)-C(3) 150.9(4); C(2)-C(3)-C(4) 135.7(4); P(1)-Ru(1)-P(3) 94.70(3); P(2)-Ru(1)-P(4) 167.75(3).

A plot of the cation [**4e**]$^+$ is shown in Figure 3. The chelating dppm ligands adopt mutually *cis*-positions, with the η$^3$-butenynyl ligand, exhibiting *E*-stereochemistry, occupying the remaining two coordination sites in the equatorial plane around the approximately octahedral cationic Ru centre. The C(1)-C(2) (1.259(5) Å) and C(3)-C(4) (1.343(5) Å) bond lengths are consistent with the butenynyl description, whilst the C(2)-C(3) (1.367(5) Å) might imply a contribution from other resonance forms.[35] The Ru-C distances fall in the range 2.136 – 2.387 Å. Structures of this type have been documented elsewhere,[35, 39-41] and merit little further comment here.

### Electrochemistry

The electrochemical responses of complexes **1 – 3** were examined by cyclic voltammetry (CV) in 0.1 M tetra-butylammonium hexafluorophosphate ([N$^n$Bu$_4$]PF$_6$) CH$_2$Cl$_2$ solutions, and quoted against ferrocene using an internal decamethylferrocene / decamethylferrocenium reference (FeCp*$_2$ / [FeCp*$_2$]$^+$ = – 0.48 V vs. FeCp$_2$ / [FeCp$_2$]$^+$) (Table 4).[42] In all cases, the first oxidation processes displayed *quasi*-reversible electrochemical behaviour at the electrode interface, with |E$_{pc}$ – E$_{pa}$| being close to that of the internal

standard at slow scan rates, but increasing with increasing scan rate. At room temperature there was evidence of EC (electrochemical-chemical) behaviour, with $i_{pa} > i_{pc}$, but with improvement to the chemical reversibility evident at reduced temperatures (– 40 °C), where current ratios approach unity.

**Table 4:** Selected electrochemical data (V) of vinylidene ([**1**]$BF_4$), *mono*-alkynyl (**2**) and *trans*-bis(alkynyl )(**3**) Ru(dppm)$_2$ complexes.

| | $E_{1/2}(1)$ | $E_{1/2}(2)$ | $E_{1/2}$(red) | $\Delta E_{1-2}$ | $\Delta E_{ox-red}$ |
|---|---|---|---|---|---|
| [**1a**]$BF_4$ | 1.07 | 1.35 | – 1.79<br>– 1.37 | 0.28 | 2.44 |
| [**1b**]$BF_4$ | 1.04 | 1.33 | – 1.13 | 0.29 | 2.17 |
| [**1c**]$BF_4$ | 0.91 | 1.28 | – 1.09 | 0.37 | 2.19 |
| [**1d**]$BF_4$ | 0.92 | 1.26 | – 1.04 | 0.34 | 1.96 |
| [**1e**]$BF_4$ | 0.84 | 1.27 | – 1.09 | 0.43 | 1.93 |
| [**1f**]$BF_4$ | 0.72 | 1.02 | – 1.17 | 0.30 | 1.89 |
| **2a** | 0.23 | 1.19 | – 1.76 | - | 1.97 |
| **2b** | 0.13 | 1.18 | - | 1.05 | - |
| **2c** | 0.06 | 1.07 | - | 1.00 | - |
| **2d** | 0.03 | 1.08 | - | 1.06 | - |
| **2e** | 0.00 | 1.03 | - | 1.03 | - |
| **2f** | – 0.08 | 0.79 | - | 0.87 | - |
| **3a** | 0.24 | 0.94 | – 1.69 | 0.70 | 1.93 |
| **3b** | 0.13 | 0.96 | - | 0.83 | - |
| **3c** | 0.06 | 1.06 | - | 1.00 | - |

The vinylidene complexes ([**1a – f**]$BF_4$) all display two oxidation events (the first *quasi*-reversible, the second irreversible; except [**1f**]$BF_4$ where both are *quasi*-reversible) and a single irreversible reduction event. The trends in $E_{1/2}(1)$, which span some 0.35 V, follow the electronic properties of the alkynyl ligand, leading to assignment of these oxidation events largely to oxidation of the phenylene fragment. In turn, $E_{1/2}(2)$ is, with the exception of [**1f**]$BF_4$, less sensitive to the nature of the R group, and is therefore assigned as a metal centred [$Ru^{II}$] / [$Ru^{III}$] oxidation. In the case of [**1f**]$BF_4$, the combination of the very strongly electron-donating OMe group and Ru(dppm)$_2$ fragment may lead to greater stabilisation of the second, possibly ligand centred, oxidation product. The reduction $E_{1/2}$(red) is attributed to reduction of the vinylidene ligand (population of the singlet carbene-like C(p) orbital at $C_\alpha$). For [**1a**]$BF_4$, R = $NO_2$, the vinylidene ligand reduction overlaps the reduction of the terminal $NO_2$ group, indicated by the higher peak current.

The *mono*-(**2**) and *bis*-(**3**) alkynyl complexes all display two oxidation events (the first *quasi*-reversible, the second irreversible; except **2f** where both oxidations are *quasi*-reversible) (Figure 4 and ESI). For **2a** reduction of the nitro group is also observed. In the case of **3a** the two nitro aromatic reductions are overlapped, evinced by the large apparent $\Delta E_p$ (190 mV). In keeping with the usual observations of the electrochemical response of ruthenium(II) alkynyl complexes, the first oxidation potential $E_{1/2}(1)$ tracks the electronic properties of the alkynyl ligand, and likely arises from depopulation of an orbital with considerable ligand character**.** The second oxidation likely has more metal character.

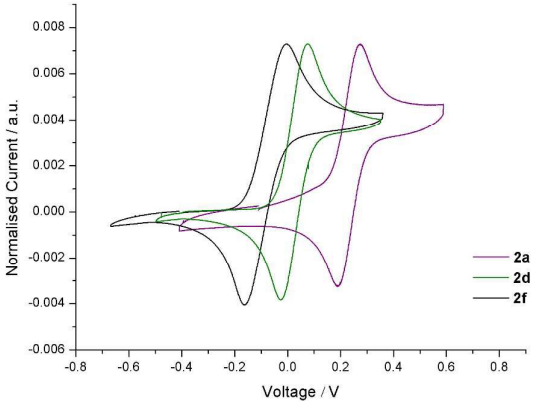


**Figure 4:** Cyclic voltammograms of representative *trans*-RuCl(C≡C$C_6H_4$-4-R)(dppm)$_2$ (**2**) complexes, where R = $NO_2$ (**2a**), H (**2d**) and OMe (**2f**). A complete figure showing the varying first oxidation potentials of **2a – f** has been included in the Supporting Information.

## Discussion

The formation, isolation and characterisation of the vinylidene complexes [**1**]$BF_4$ and *mono*-alkynyl complexes **2** allowed the sequence of events leading to the formation of *trans*-bis(alkynyl) complexes **3** vs. the $\eta^3$-butenynyl complexes [**4**]$BF_4$ to be followed by *in situ* $^{31}P\{^1H\}$ NMR spectroscopy. From a mixture of *cis*-$RuCl_2$(dppm)$_2$ $TlBF_4$, HC≡C$C_6H_4$-4-R and 1,8-*bis*-dimethylaminonaphthalene in $CH_2Cl_2$ solutions, the *mono*-alkynyl complexes **2** (s, *ca.* δ – 7.0 ppm) begin to form within 5 minutes. As the reaction proceeds, the complexes **2** react further to give the *trans*-bis(alkynyl) complexes **3** (s, *ca.* δ – 4.0 ppm). For cases when the R substituent is electron withdrawing (Figure 5), **3** were ultimately formed without any appreciable by-products. However, when the R substituent is electron donating (Figure 6), before complete conversion of **2** to **3**, the $\eta^3$-butenynyl complex [**4**]$^+$ is observed with four new $^{31}P\{^1H\}$ NMR resonances in a characteristic ABMX coupling pattern.[35] As the reaction proceeds, the product distribution shifts to give the $\eta^3$-butenynyl species cleanly without any appreciable by-products, implying the intermediacy of **3** in the formation of [**4**]$^+$.

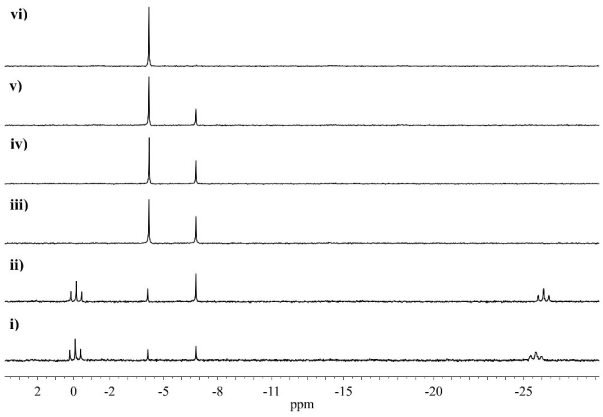


**Figure 5**: *In situ* $^{31}P\{^{1}H\}$ NMR solution spectroscopy monitoring of *cis*-$RuCl_2(dppm)_2$, $TlBF_4$ (2 equiv.), $HC{\equiv}CC_6H_4$-4-COOMe (2.2 equiv.), 1,8-*bis*-dimethylaminonapthalene (excess), $CH_2Cl_2$: i) 5 min; ii) 20 min; iii) 1 hr; iv) 3 hr; v) 7 hr; vi) 30 hr.

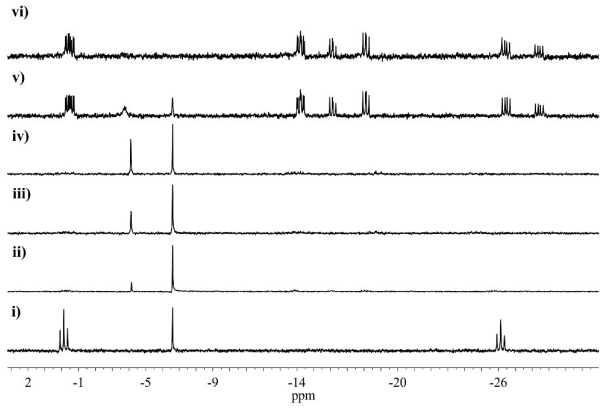


**Figure 6**: *In situ* $^{31}P\{^{1}H\}$ NMR solution spectroscopy of *cis*-$RuCl_2(dppm)_2$, $TlBF_4$ (2 equiv.), $HC{\equiv}CC_6H_4$-4-Me (2.2 equiv.), 1,8-*bis*-dimethylaminonapthalene (excess), $CH_2Cl_2$: i) 5 min; ii) 75 min; iii) 2 hr; iv) 3 hr; v) 24 hr; vi) 48 hr.

In the cases where R is an electron donating group, attempts were made to purify the reaction mixture at intermediate times and isolate the spectroscopically observed intermediate *trans*-bis(alkynyl) complexes. These attempts were unsuccessful, yielding only the $\eta^3$-butenynyl complex, $[\mathbf{4}]^+$ suggesting that the *trans*-bis(alkynyl) complexes undergo further reaction on work-up. Notably upon extending the reaction time leading to the formation of **3b** to 48 hours, minor amounts of the corresponding $\eta^3$-butenynyl complex was also observed in solution. Though the formation of complexes of the general type **2**,[28-31, 36, 43-47] **3**[19, 31, 37, 48-50] and $[\mathbf{4}]^+$ [51-55] is not uncommon, the role of the incoming alkyne in the transformations to these complexes has not been explored in detail.[56]

A mechanism for the formation of $\eta^3$-butenynyl complexes from $[\mathbf{1d}]^+$ in methanol has recently been proposed, based on spectroscopic evidence for the intermediates **A** and **B** (Scheme 3).[35] In the case of reactions reported here, no spectroscopic evidence for either **A** or **B** could be obtained (Figure 5, Figure 6). Rather deprotonation of the vinylidene complexes $[\mathbf{1}]^+$ affords alkynyls **2** and subsequent reaction with the efficient halide abstracting agent $TlBF_4$ presumably forms the five coordinate species $[\mathbf{E}]^+$, which in the presence of a terminal alkyne and excess 1,8-*bis*-dimethylaminonaphthalene gives **3**, likely *via* the intermediate alkynyl-vinylidene species $[\mathbf{F}]^+$ (Scheme 4).

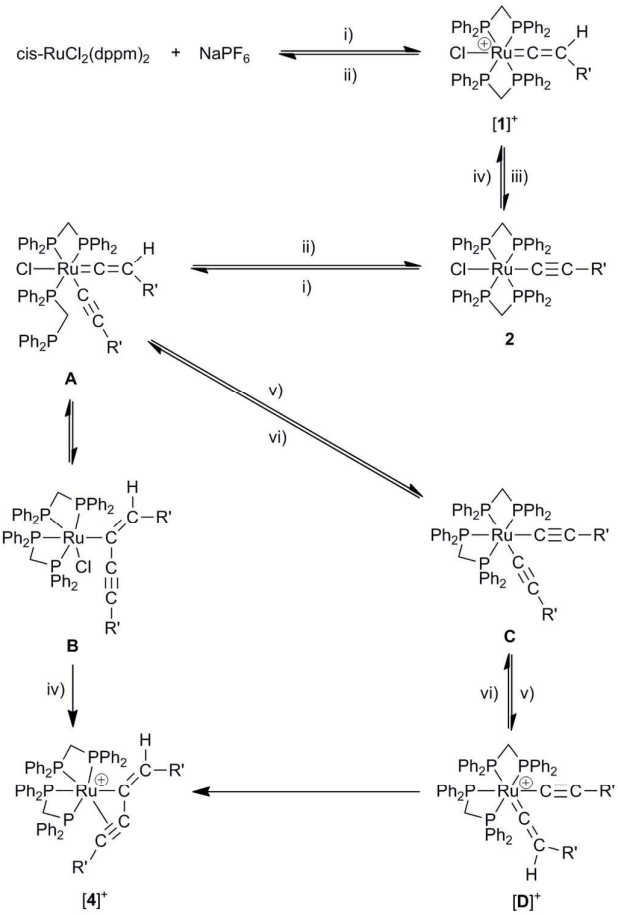


**Scheme 3**: Proposed mechanism for the reaction of *cis*-$RuCl_2(dppm)_2$, $NaPF_6$, $HC{\equiv}CC_6H_5$ and base, where: i) + $HC{\equiv}CC_6H_5$; ii) – $HC{\equiv}CC_6H_5$; iii) – $H^+$; iv) + $H^+$; v) – HCl; vi) + HCl; vii) – Cl and R´ = $C_6H_5$.

From **3**, it is possible to envision two alternate routes to $[\mathbf{4}]^+$ (Scheme 4), either *via* the reverse reaction to give $[\mathbf{F}]^+$ and isomerisation to the key *cis*-alkynyl vinylidene $[\mathbf{D}]^+$ or through initial isomerisation to the *cis*-*bis*(alkynyl) complex **C** prior to protonation to give $[\mathbf{D}]^+$. The route **3** → $[\mathbf{F}]^+$ → $[\mathbf{D}]^+$ → $[\mathbf{4}]^+$ is similar to that proposed by Rappert and Yamamoto to account for the formation of butenynyl complexes from *trans*-

$Ru(C{\equiv}CC_6H_5)_2(PMe_3)_4$,[57] whilst the formation of $\eta^3$-butenynyl complexes from **C** (Scheme 3, 4) is similar to the formation of butenynyl complexes from *cis*-$Ru(C{\equiv}CC_6H_5)_2\{P(CH_2CH_2PPh_2)_3\}$ with weak acids ($NH_4^+$, $pK_a$ = 9; EtOH, $pK_a$ 18; *c.f.* $pK_a$ 1-dimethylamino-8-dimethylaminium-naphthalene 12.1[58] (water) – 18.62[59] (NCMe) observed by Bianchini and colleagues.[60]

In order to gain further insight into these different mechanistic possibilities and also to rationalise the observed substituent effects, the potential energy surface for the formation of $[\mathbf{4}]^+$ was examined using DFT methods at the PBE0-D3/def2-TZVPP//BP86/SV(P) level with solvation corrections applied in $CH_2Cl_2$. All energies are Gibbs energies at 298.15 K. Alkynyl ligands with three different substituents (-$C_6H_4$-4-$NO_2$, **a**; -$C_6H_5$, **d** and -$C_6H_4$-4-OMe, **f**) were examined and in each case, the alkynyl/vinylidene complex $[\mathbf{D}]^+$ was taken as the reference point.

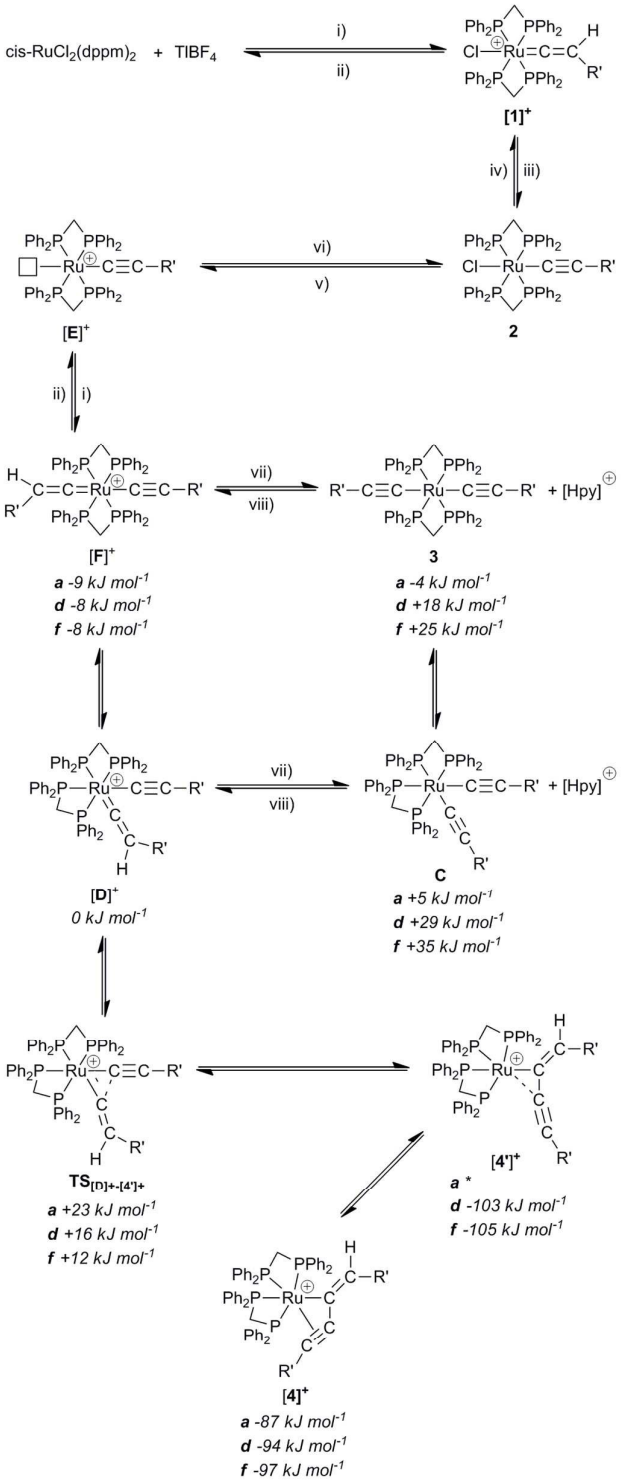


**Scheme 4**: Proposed mechanism for the reaction of *cis*-$RuCl_2(dppm)_2$, $TlBF_4$, $HC{\equiv}CC_6H_4$-4-R and base, where: i) + $HC{\equiv}CC_6H_4$-4-R; ii) – $HC{\equiv}CC_6H_4$-4-R; iii) – H; iv) + H v) – Cl; vi) + Cl; vii) + pyridine; viii) – pyridine and R' = $C_6H_4$-4-R.(**a** R = $NO_2$, **d** R = H, **f** R = OMe) DFT-calculated free energies at 298.15 K are shown in italics. * geometry optimisation resulted in $[\mathbf{4a}]^+$.

The calculations indicate that in the case of the *bis*-alkynyl and alkynyl/vinylidene complexes, the *trans*-isomers (**3** and $[\mathbf{F}]^+$)

are more thermodynamically favourable than the corresponding *cis*-arrangement of ligands (**C** and $[\mathbf{D}]^+$), although the differences are relatively small (*ca.* 10 kJ mol$^{-1}$). The isomerisation of $[\mathbf{F}]^+$ to $[\mathbf{D}]^+$, and **3** to **C** was not modelled, but is thought to proceed through a five-coordinate intermediate with a $\kappa^1$-bound dppm ligand.[35] In order to assess the differences in acidity of the vinylidene ligands, deprotonation of the cationic complexes $[\mathbf{D}]^+$ and $[\mathbf{F}]^+$ by pyridine (to give a pyridinium cation and complexes **C** and **3** respectively) was modelled (For details of deprotonation by other bases, see Supporting Information). The data indicate that in all cases except **3a**, deprotonation of the vinylidene ligand in $[\mathbf{F}]^+$ by pyridine is thermodynamically unfavourable. There is a pronounced substituent effect with the greatest difference in energy between the (less favourable) *trans*-bis(alkynyl) complexes **3** and the alkynyl/vinylidene species $[\mathbf{F}]^+$ arising when two OMe substituents are present (**f**). The energy difference is much smaller in the $NO_2$-containing case (**a**). This trend may simply represent the increased basicity of the alkynyl ligands in the presence of the OMe group.

The formation of the $\eta^3$-butenynyl ligand from intermediate $[\mathbf{D}]^+$ proceeds through a low energy transition state, $\mathbf{TS}_{[\mathbf{D}]+-[\mathbf{4'}]+}$ (Scheme 4). There is a small substituent effect in this case with the barrier to C-C bond formation in the transition state being lowest in the case of the OMe-substituted complex **f** ($\Delta G$ = +12 kJ mol$^{-1}$) and greatest in the case of the $NO_2$-derviative **a** ($\Delta G$ = +23 kJ mol$^{-1}$). This is consistent with the relative nucleophilicity of the alkynyl ligands coupling with the electrophilic metal-bound carbon of the vinylidene. However, given that the barriers are very small, the calculations predict that the C-C bond formation step from $[\mathbf{D}]^+$ will be extremely rapid at 298 K, regardless of the substituent employed. The observed experimental substituent effect, where the presence of electron-donating groups favours the formation of the butenynyl-containing complexes, may be more readily explained on the basis of the protonation states of the complexes. The presence of the more basic (OMe-containing) alkynyl ligand will increase the proportion of butenynyl/vinylidene complexes $[\mathbf{F}]^+$ and $[\mathbf{D}]^+$ thus promoting the formation of $[\mathbf{4}]^+$, whereas in the case of the $NO_2$-containing species, the proportion of these species will be lower, hence a much slower formation of the butenynyl complex.

One additional aspect of the calculation is that a dynamic reaction coordinate (DRC) analysis of $\mathbf{TS}_{[\mathbf{D}]-[\mathbf{4'}]+}$ (and also the corresponding Z-isomer) reveals that the transition state does not directly connect $[\mathbf{D}]^+$ to $[\mathbf{4}]^+$ but to an isomeric complex, $[\mathbf{4'}]^+$ in which the butenynyl ligand is bound in an $\eta^1$-fashion. At all levels of theory employed $[\mathbf{4'}]^+$ is lower in energy than $[\mathbf{4}]^+$ for the hydrogen- and methoxy-substituted complexes, by 9 and 8 kJ mol$^{-1}$ respectively. Geometry optimisation of the corresponding $NO_2$-substituted species resulted in generation of $[\mathbf{4a}]^+$. Although the energy differences here are small and so care should be taken in interpreting these data, the calculations would indicate that $[\mathbf{4}]^+$ and $[\mathbf{4'}]^+$ should both be in equilibrium in solution. This is consistent with the fact that the alkyne functionality in butenynyl ligands is labile and may be readily replaced by donor ligands such as CO.[39]

The calculations also explain the stereochemical outcome of the reaction as the *E*-substituted butenynyl ligand is obtained. As shown in Scheme 5, the calculations indicate that the intermediates and transition states which lead to the alternative *Z*-isomer $[\mathbf{4d}\text{-}\boldsymbol{Z}]^+$ ($[\mathbf{Dd}\text{-}\boldsymbol{Z}]^+$ and $\mathbf{TS}_{[\mathbf{Dd}\text{-}\boldsymbol{Z}]+-[\mathbf{4d}\text{-}\boldsymbol{Z}]+}$) are only slightly higher in energy than the corresponding species which lead to the experimentally observed *E*-isomer (by 9 and 6 kJ mol$^{-1}$ respectively) (Scheme 5). However, the *Z*-isomer of complex $[\mathbf{4d}]^+$, $[\mathbf{4d}\text{-}\boldsymbol{Z}]^+$ is at far higher energy than the *E*-isomer (– 47 kJmol$^{-1}$ compared to – 94 kJ mol$^{-1}$) as is $[\mathbf{4'd}\text{-}\boldsymbol{Z}]^+$ (– 62 kJ mol$^{-1}$, versus – 103 kJ mol$^{-1}$ for $[\mathbf{4d}]^+$). This implies that the reverse reaction from $[\mathbf{4'd}\text{-}\boldsymbol{Z}]^+$ to $[\mathbf{Dd}\text{-}\boldsymbol{Z}]^+$ has a barrier of 84 kJ mol$^{-1}$ and may be reversible at 298 K, implying that the reaction is under thermodynamic control.

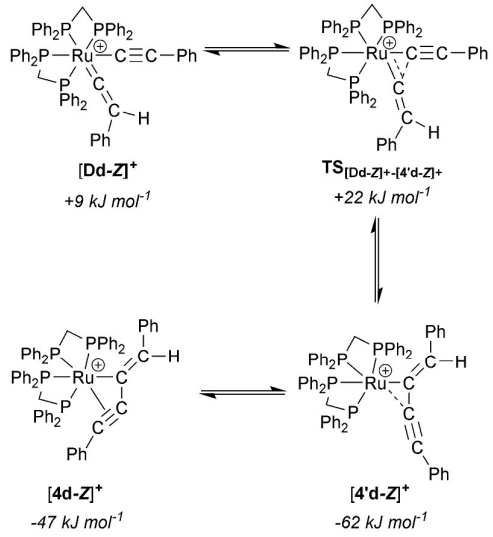


**Scheme 5:** Proposed mechanism for the formation of the *Z*-isomer of the butenynyl complex $[\mathbf{4d}\text{-}\boldsymbol{Z}]^+$. DFT-calculated free energies at 298.15 K are shown in italics.

## Conclusions

In summary, $TlBF_4$ has been shown to be a reliable and efficient halide abstracting agent in the transformation of *cis*-$RuCl_2(dppm)_2$ into vinylidene and alkynyl complexes. Although *trans*-bis(alkynyl) complexes, *trans*-$Ru(C{\equiv}CC_6H_4\text{-}4\text{-}R)_2(dppm)_2$, can be obtained from terminal alkynes $HC{\equiv}CC_6H_4$-4-R containing electron withdrawing R substituents, terminal alkynes containing electron donating R substituents promote further reaction to give cationic $\eta^3$-butenynyl complexes $[Ru(\eta^3\text{-}\{HC(C_6H_4\text{-}4\text{-}R){=}CC{\equiv}CC_6H_4\text{-}4\text{-}R\})(dppm)_2]BF_4$. Although electron donating R substituents increase the nucleophilicity at $C^1$ in the incoming alkyne, $HC^1{\equiv}C^2C_6H_4$-4-R, which increases the nucleophilicity and electrophilicity of the alkynyl and vinylidene $C_\alpha$ carbons (respectively) in the intermediate alkynyl-vinylidene complexes, it appears that it is the control of the protonation state by raising the energy of the *bis*-

alkynyl complex which promotes the formation of the $\eta^3$-butenynyl complexes.

## Acknowledgements

S.G.E. gratefully acknowledges the award of a University of Durham Doctoral Scholarship. P.J.L. holds an Australian Research Council Future Fellowship (FT120100073) gratefully acknowledges funding from the Australian Research Council (DP140100855). We are grateful to the Royal Society of Chemistry for the award of a Journals Grant for International Authors to J.M.L., which greatly assisted this project. This work was further supported by the EPSRC (Grants GR/H011455/1 and EP/K031589/1). The authors acknowledge the facilities, and the scientific and technical assistance of the Australian Microscopy & Microanalysis Research Facility at the Centre for Microscopy, Characterisation & Analysis, The University of Western Australia, a facility funded by the University, State and Commonwealth Governments.

## Notes and references

1. S. Marqués-González, M. Parthey, D. S. Yufit, J. A. K. Howard, M. Kaupp and P. J. Low, *Organometallics*, 2014.
2. Y. Liu, C. M. Ndiaye, C. Lagrost, K. Costuas, S. Choua, P. Turek, L. Norel and S. Rigaut, *Inorg. Chem.*, 2014, **53**, 8172.
3. E. Wuttke, Y.-M. Hervault, W. Polit, M. Linseis, P. Erler, S. Rigaut and R. F. Winter, *Organometallics*, 2014, **33**, 4672.
4. G. Grelaud, N. Gauthier, Y. Luo, F. Paul, B. Fabre, F. Barriere, S. Ababou-Girard, T. Roisnel and M. G. Humphrey, *J. Phys. Chem. C*, 2014, **118**, 3680.
5. L. Luo, A. Benameur, P. Brignou, S. H. Choi, S. Rigaut and C. D. Frisbie, *J. Phys. Chem. C*, 2011, **115**, 19955.
6. A. Vacher, F. Barrière and D. Lorcy, *Organometallics*, 2013, **32**, 6130.
7. K. Costuas and S. Rigaut, *Dalton Trans*, 2011, **40**, 5643.
8. C. Olivier, B. Kim, D. Touchard and S. Rigaut, *Organometallics*, 2008, **27**, 509.
9. B. Kim, J. M. Beebe, C. Olivier, S. Rigaut, D. Touchard, J. G. Kushmerick, X. Y. Zhu and C. D. Frisbie, *J. Phys. Chem. C*, 2007, **111**, 7521.
10. J.-W. Ying, Z. Cao, C. Campana, Y. Song, J.-L. Zuo, S. F. Tyler and T. Ren, *Polyhedron*, 2015, **86**, 76.
11. D. Touchard, C. Morice, V. Cadierno, P. Haquette, L. Toupet and P. H. Dixneuf, *J. Chem. Soc., Chem. Commun.*, 1994, 859.
12. D. Touchard, P. Haquette, A. Daridor, A. Romero and P. H. Dixneuf, *Organometallics*, 1998, **17**, 3844.
13. M. A. Fox, J. E. Harris, S. Heider, V. Pérez-Gregorio, M. E. Zakrzewska, J. D. Farmer, D. S. Yufit, J. A. K. Howard and P. J. Low, *J. Organomet. Chem.*, 2009, **694**, 2350.
14. S. Guesmi, D. Touchard and P. H. Dixneuf, *Chemical Communications*, 1996, 2773.
15. B. Chin, A. J. Lough, R. H. Morris, C. T. Schweitzer and C. D'Agostino, *Inorg. Chem.*, 1994, **33**, 6278.
16. P. J. Low, *Coord. Chem. Rev.*, 2013, **257**, 1507.
17. N. Tuccitto, V. Ferri, M. Cavazzini, S. Quici, G. Zhavnerko, A. Licciardello and M. A. Rampi, *Nat Mater*, 2009, **8**, 41.
18. F. Schwarz, G. Kastlunger, F. Lissel, H. Riel, K. Venkatesan, H. Berke, R. Stadler and E. Lörtscher, *Nano Letters*, 2014, **14**, 5932.
19. K. Liu, X. Wang and F. Wang, *ACS Nano*, 2008, **2**, 2315.
20. F. Lissel, F. Schwarz, O. Blacque, H. Riel, E. Loertscher, K. Venkatesan and H. Berke, *J. Am. Chem. Soc.*, 2014, **136**, 14560.
21. P. J. Low, *Dalton Trans*, 2005, 2821.
22. F. Lissel, F. Schwarz, O. Blacque, H. Riel, E. Lörtscher, K. Venkatesan and H. Berke, *J. Am. Chem. Soc.*, 2014, **136**, 14560.
23. Z. Cao, B. Xi, D. S. Jodoin, L. Zhang, S. P. Cummings, Y. Gao, S. F. Tyler, P. E. Fanwick, R. J. Crutchley and T. Ren, *J. Am. Chem. Soc.*, 2014, **136**, 12174.
24. S. Marques-Gonzalez, D. S. Yufit, J. A. K. Howard, S. Martin, H. M. Osorio, V. M. Garcia-Suarez, R. J. Nichols, S. J. Higgins, P. Cea and P. J. Low, *Dalton Trans*, 2013, **42**, 338.
25. G. Kastlunger and R. Stadler, *Phys. Rev. B*, 2014, **89**.
26. E. Wuttke, F. Pevny, Y.-M. Hervault, L. Norel, M. Drescher, R. F. Winter and S. Rigaut, *Inorg. Chem.*, 2012, **51**, 1902.
27. F. Lissel, T. Fox, O. Blacque, W. Polit, R. F. Winter, K. Venkatesan and H. Berke, *J. Am. Chem. Soc.*, 2013, **135**, 4051.
28. D. Touchard, P. Haquette, N. Pirio, L. Toupet and P. H. Dixneuf, *Organometallics*, 1993, **12**, 3132.
29. P. Haquette, N. Pirio, D. Touchard, L. Toupet and P. H. Dixneuf, *J. Chem. Soc., Chem. Commun.*, 1993, 163.
30. M. C. B. Colbert, J. Lewis, N. J. Long, P. R. Raithby, M. Younus, A. J. P. White, D. J. Williams, N. N. Payne, L. Yellowlees, D. Beljonne, N. Chawdhury and R. H. Friend, *Organometallics*, 1998, **17**, 3034.
31. C. W. Faulkner, S. L. Ingham, M. S. Khan, J. Lewis, N. J. Long and P. R. Raithby, *J. Organomet. Chem.*, 1994, **482**, 139.
32. Z. Atherton, C. W. Faulkner, S. L. Ingham, A. K. Kakkar, M. S. Khan, J. Lewis, N. J. Long and P. R. Raithby, *J. Organomet. Chem.*, 1993, **462**, 265.
33. M. Younus, N. J. Long, P. R. Raithby, J. Lewis, N. A. Page, A. J. P. White, D. J. Williams, M. C. B. Colbert, A. J. Hodge, M. S. Khan and D. G. Parker, *J. Organomet. Chem.*, 1999, **578**, 198.
34. J. Chatt and R. G. Hayter, *J. Chem. Soc.*, 1961, 896.
35. J. M. Lynam, T. D. Nixon and A. C. Whitwood, *J. Organomet. Chem.*, 2008, **693**, 3103.
36. A. J. Hodge, S. L. Ingham, A. K. Kakkar, M. S. Khan, J. Lewis, N. J. Long, D. G. Parker and P. R. Raithby, *J. Organomet. Chem.*, 1995, **488**, 205.
37. A. M. McDonagh, I. R. Whittall, M. G. Humphrey, D. C. R. Hockless, B. W. Skelton and A. H. White, *J. Organomet. Chem.*, 1996, **523**, 33.
38. (a) J. E. McGrady, T. Lovell, R. Stranger and M. G. Humphrey, *Organometallics*, 1997, **16**, 4004. (b) J. Manna, K.D. John, M.D. Hopkins, *Adv. Organomet. Chem.*, 1995, **38**, 79-154.
39. C. Bianchini, M. Peruzzini, F. Zanobini, P. Frediani and A. Albinati, *J. Am. Chem. Soc.*, 1991, **113**, 5453.
40. G. Jia, A. L. Rheingold and D. W. Meek, *Organometallics*, 1989, **8**, 1378.

41. C. Bianchini, P. Innocenti, M. Peruzzini, A. Romerosa and F. Zanobini, *Organometallics*, 1996, **15**, 272.
42. N. G. Connelly and W. E. Geiger, *Chem. Rev.*, 1996, **96**, 877.
43. A. M. McDonagh, I. R. Whittall, M. G. Humphrey, B. W. Skelton and A. H. White, *J. Organomet. Chem.*, 1996, **519**, 229.
44. N. J. Long, A. J. Martin, F. F. de Biani and P. Zanello, *J. Chem. Soc. Dalton Trans.*, 1998, 2017.
45. A. M. McDonagh, N. T. Lucas, M. P. Cifuentes, M. G. Humphrey, S. Houbrechts and A. Persoons, *J. Organomet. Chem.*, 2000, **605**, 193.
46. S. K. Hurst, M. P. Cifuentes, J. P. L. Morrall, N. T. Lucas, I. R. Whittall, M. G. Humphrey, I. Asselberghs, A. Persoons, M. Samoc, B. Luther-Davies and A. C. Willis, *Organometallics*, 2001, **20**, 4664.
47. B. Babgi, L. Rigamonti, M. P. Cifuentes, T. C. Corkery, M. D. Randles, T. Schwich, S. Petrie, R. Stranger, A. Teshome, I. Asselberghs, K. Clays, M. Samoc and M. G. Humphrey, *J. Am. Chem. Soc.*, 2009, **131**, 10293.
48. M. Younus, N. J. Long, P. R. Raithby, J. Lewis, N. A. Page, A. J. P. White, D. J. Williams, M. C. B. Colbert, A. J. Hodge, M. S. Khan and D. G. Parker, *J. Organomet. Chem*, 1999, **578**, 198.
49. A. M. McDonagh, M. P. Cifuentes, I. R. Whittall, M. G. Humphrey, M. Samoc, B. Luther-Davies and D. C. R. Hockless, *J. Organomet. Chem.*, 1996, **526**, 99.
50. H. W. Lin, X. H. Wang, X. J. Zhao, J. Li and F. S. Wang, *Synth. Met.*, 2003, **135–136**, 239.
51. G. C. Jia, J. C. Gallucci, A. L. Rheingold, B. S. Haggerty and D. W. Meek, *Organometallics*, 1991, **10**, 3459.
52. G. Albertin, P. Amendola, S. Antoniutti, S. Ianelli, G. Pelizzi and E. Bordignon, *Organometallics*, 1991, **10**, 2876.
53. A. Dobson, D. S. Moore, S. D. Robinson, M. B. Hursthouse and L. New, *Polyhedron*, 1985, **4**, 1119.
54. G. Albertin, S. Autoniutti, E. Bordignon, F. Cazzaro, S. Ianelli and G. Pelizzi, *Organometallics*, 1995, **14**, 4114.
55. L. D. Field, A. V. George, G. R. Purches and I. H. M. Slip, *Organometallics*, 1992, **11**, 3019.
56. O. J. S. Pickup, I. Khazal, E. J. Smith, A. C. Whitwood, J. M. Lynam, K. Bolaky, T. C. King, B. W. Rawe and N. Fey, *Organometallics*, 2014, **33**, 1751.
57. T. Rappert and A. Yamamoto, *Organometallics*, 1994, **13**, 4984.
58. D. Banerjee, Z. Hu and J. Li, *Dalton Trans.*, 2014, **43**, 10668.
59. I. Kaljurand, A. Kütt, L. Sooväli, T. Rodima, V. Mäemets, I. Leito and I. A. Koppel, *J. Org. Chem.*, 2005, **70**, 1019.
60. C. Bianchini, P. Frediani, D. Masi, M. Peruzzini and F. Zanobini, *Organometallics*, 1994, **13**, 4616.

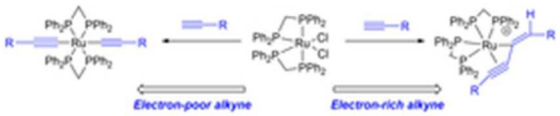


The course of reactions between cis-RuCl2(dppm)2 and terminal alkynes is shown to depend markedly on the electronic character of the alkyne reagent.
23x4mm (300 x 300 DPI)